ISSN: 1992-8645 www.jatit.org E-ISSN: 1817-3195

UNCOVERING THE INTRINSIC NATURE OF TRAFFIC OSCILLATIONS: AN EMPIRICAL AND SIMULATION-BASED APPROACH

AHLAM EL ATTARI[1], KAMAL JETTO[2], ZINEB TAHIRI[3], ABDELILAH BENYOUSSEF[4], ABDALLAH EL KENZ[5]

[1]PhD Student, Laboratoire De Matière Condensée Et Sciences Interdisciplinaires, Département De Physique, Faculté Des Sciences, Université Mohammed V, Rabat, Morocco

[2]Full Professor and Head of Department of Logistics and Transportation, Research Team Transport, Logistics And Road Safety, Ecole Hassania Des Travaux Publics, Km 7 Route D'El Jadida, B.P 8108, Oasis Casablanca, Morocco

[3]Assistant Professor, Department of Logistics and Transportation, Research Team Transport, Logistics and Road Safety, Ecole Hassania Des Travaux Publics, Km 7 Route D'El Jadida, B.P 8108, Oasis Casablanca, Morocco

[4]Full Professor, Laboratoire De Matière Condensée Et Sciences Interdisciplinaires, Département De Physique, Faculté Des Sciences, Université Mohammed V, Rabat, Morocco, Hassan II Academy Of Science And Technology, Rabat, Morocco

[5]Full Professor, Laboratoire De Matière Condensée Et Sciences Interdisciplinaires, Département De Physique, Faculté Des Sciences, Université Mohammed V, Rabat, Morocco

E-mail: [1]ahlam_elattari@um5.ac.ma, [2]jettkam@gmail.com, [3]tahiri.zineb@ehtp.ac.ma, [4]a.benyoussef@um5r.ac.ma, [5]elkenz@fsr.ac.ma

ABSTRACT

This paper challenges the conventional understanding of traffic oscillations, traditionally associated with congested conditions and minor disturbances. Through empirical analysis of diverse datasets, we demonstrate that traffic oscillations persist across various traffic states, conditions, and road section types. By applying curve fitting techniques to key traffic observables (space headway, time headway, and mean velocity), we quantified these oscillations and determined their characteristic periods. In free flow and jam states, the period corresponds to the average vehicle travel time (T_0), while in congested conditions, it equals $2\pi\tau$, where τ represents the relaxation time. To complement empirical findings, we employed Cellular Automata models, specifically the NaSch model, which allowed for parameter adjustment to simulate diverse traffic conditions. This approach corroborated empirical results and revealed that oscillation frequency in free flow is determined solely by maximum speed, while in jammed states, it depends exclusively on traffic density. These findings suggest that traffic oscillations are an intrinsic property of traffic flow dynamics, rather than merely a product of human behavior. Furthermore, this study establishes vehicle travel time as an effective metric for analyzing traffic flow in stable, homogeneous conditions.

Keywords: *Traffic Oscillation, Traffic Oscillations Period, Traffic Flow Dynamics, Empirical Analysis, Cellular Automata Models.*

1. INTRODUCTION:

Traffic oscillations can be defined as temporal fluctuations in traffic variables such as flow and speed. they have become a focal point in contemporary transportation research due to their significant impact on road efficiency. Typically observed in congested traffic conditions, these fluctuations can propagate upstream, forming what are commonly known as "stop-and-go waves", where vehicles alternate between moving freely and being halted in traffic jams [1,2,3,4,5,6,33].

Traffic oscillations have a profound impact on the performance and safety of road networks. These fluctuations in traffic flow diminish the overall road capacity, as the stop-and-go waves prevent vehicles from utilizing the available road space [2]. This reduction in road efficiency can lead to longer travel times and increased congestion, frustrating and stressing drivers and impacting their productivity. Moreover, the frequent speed changes associated with traffic oscillations increases the risk of vehicular collisions [6]. As drivers repeatedly transition between acceleration and braking, the probability of rear-end collisions and other accidents increases, particularly when reaction times are compromised due to fatigue, distraction, or stress. The environmental consequences of the traffic oscillations are equally concerning. The acceleration and deceleration cycles force vehicles to operate inefficiently, resulting in elevated fuel consumption and, consequently, higher levels of greenhouse gas emissions [7]. This not only contributes to increased operational costs for drivers but also aggravates the environmental pollution and climate change concerns

Various theories have been proposed to explain the formation and propagation of traffic oscillations. From both physical and mathematical perspectives [8], these oscillations are attributed to system instability, whether linear or non-linear [32,10,11,13].

The linear instability theory suggests that small disturbances in traffic flow can grow over time due to the inherent instability of the traffic system [1,2]. These disturbances, caused by variations in driver behavior or external factors, propagate and amplify, leading to the formation of stop-and-go waves. Whilst the non-linear dynamics consider the complex interactions between vehicles and the resulting feedback loops [3,4,5]. In this view, traffic oscillations emerge from non-linear interactions within the traffic stream, where even minor changes in speed or distance between vehicles can lead to large-scale oscillatory patterns.

In contrast, a behavioral car-following model was developed [2,8], building on Newell's car-following model [14], to describe the underlying mechanism. This model accounts for human driver behavior and how it influences traffic flow. The extended model incorporates elements like driver reaction time, acceleration, and deceleration behaviors, offering a more comprehensive explanation of how individual driver actions contribute to the formation and propagation of traffic oscillations [6]. Early observations by transportation researchers, who noted the non-linear and often chaotic behavior of traffic under congested conditions, stated that one of the foundational works in this area is the concept of "phantom traffic jams" where traffic waves spontaneously form without any apparent external cause [15,10,16,17]. It was also discussed that sudden reductions in roadway capacity, such as those caused by lane reductions or accidents, can induce traffic oscillations [18]. As vehicles approach these bottlenecks, the abrupt change in driving conditions leads to waves of slowing and accelerating traffic [15].

Empirical studies on traffic oscillations provide valuable insights into the characteristics and dynamics of these phenomena in real-world traffic conditions. These studies often utilize traffic data to observe and analyze oscillations, focusing on their formation, propagation, and impact on traffic flow. It has been observed that traffic oscillations commonly form at bottlenecks and propagate upstream, characterized by cyclic patterns of deceleration and acceleration. An international comparison of freeway traffic oscillations in different countries revealed variations in oscillation characteristics. While traffic oscillations are consistent across all studied locations, the oscillation angular frequency is likely site-specific. General differences between the frequencies measured in different countries have yet to be conclusively identified [39,19]. Researchers also examined the effects of merging and diverging traffic on freeway oscillations, showing that these actions exacerbate oscillation formation, growth, and propagation [20]. In other words, this theory states that merging and/or diverging flows change in response to freeway oscillations and these changes in flow leads to the damping or the amplification of oscillations.

Traffic researchers have proposed several strategies to mitigate the effects of traffic oscillations aiming to create smoother, more predictable traffic flow and reduce the frequency and amplitude of these waves. Adaptive traffic signal systems represent one of the technological solutions. These intelligent systems use real-time data from sensors and cameras to adjust signal timing dynamically to respond to the actual traffic conditions rather than relying on pre-programmed cycles in order to help maintain a more consistent flow of vehicles, potentially reducing the likelihood of oscillations forming [8]. The integration of autonomous vehicles (AVs) into traffic streams has been a focus of recent research, with their ability to maintain consistent speeds and optimal following distances, that could act as stabilizing elements in traffic flow. These experiments have given intriguing results, suggesting that AVs could have an impact on smoothing traffic flow. One notable study by Stern et al. (2018) [4] demonstrated that the control of a single autonomous vehicle within a traffic stream could significantly reduce the amplitude of oscillations. This intervention led to a smoother traffic flow, which in turn resulted in measurable reductions in fuel consumption and emissions across all vehicles in the system.

However, it is crucial to note that these technological solutions face a significant challenge: the unpredictability of human behavior. A driver who suddenly decides to change lanes, brake unnecessarily, or accelerate aggressively can trigger a chain reaction that leads to oscillations, regardless of the technological systems in place [10]. In other words, the complex interactions between human drivers, varying road conditions, and external factors continue to generate and sustain these oscillations.

Previous studies on traffic oscillations have predominantly focused on congested conditions, attributing oscillations to traffic instabilities, driver behavior, or bottleneck effects. However, little attention has been given to oscillations that occur in other traffic states such as free flow and jam conditions. This leaves an important gap in understanding whether oscillations are confined to congestion or represent a more fundamental property of traffic dynamics. Motivated by this gap, our study investigates oscillations across all traffic states and evaluates whether they are intrinsic to traffic flow.

In closing, these oscillations diminish road capacity, increase collision risks, and elevate fuel consumption, contributing to environmental pollution. Various theories, such as linear instability and non-linear dynamics, have been proposed to explain the formation of these oscillations, while recent research suggests that strategies like adaptive traffic signals and the integration of autonomous vehicles can mitigate their effects, leading to smoother traffic flow and reduced emissions. Despite significant progress, several aspects of traffic oscillations remain poorly understood or are subjects of ongoing investigation. Key questions include:

1) Traffic States: Can oscillations be observed in non-congested traffic states? Do these oscillations depend on the traffic state and the nature of the road section?

2) Oscillation Frequency: Is there a universal formula for oscillation frequency?

3) Frequency Dependence: Does the angular frequency of oscillations depend on specific traffic parameters?

4) Model Validation: Can existing traffic models accurately reproduce and prove the existence of traffic oscillations? if yes can we consider these oscillations to be an intrinsic traffic phenomenon?

In this paper we will try to address these questions to understand these oscillations and try to formulate effective strategies to reduce traffic oscillations and improve overall traffic system performance. Indeed, we believe that the characteristics of those oscillations should be revealed. Thus, we address the influence of traffic system parameters on those characteristics.

2. METHODOLOGY:

in this section we will give a brief presentation of the datasets and models that we have used in this analysis and the steps done to achieve the results.

2.1 *Empirical Analysis:*

Datasets were chosen from the federal highway administration's (FHWA) next generation simulation (NGSIM) project (US. department of transportation federal highway administration). It is worth to say that this database is considered one of the most comprehensive and widely used datasets in traffic flow research. It provides 45-minute datasets segmented into three 15-minute periods:

- Interstate-80 in Emeryville, California, on April 13,2005, (I-80-1 – I-80-2 – I-80-3) collected between 4: 00p.m to 4: 15p.m and 5: 00p.m to 5:30p.m. the studied section is approximately 500 meters long and consists of six freeway lanes, including a high-occupancy vehicle (HOV) lane and an on-ramp.

- Freeway US-101 in Los Angeles, California, on April 13, 2005, (US101-1 – US101-2 – US101-3) collected between 7: 50p.m to 8: 35p.m.the studied section is approximately 640 meters and consists of five main lanes thought the section, including an on-ramp and an off-ramp.

These real-world datasets consist of detailed vehicles trajectories obtained from analyzing footage, collected using multiple synchronized digital video cameras, of the vehicles passing through the studied area. This vehicle trajectory data provided the precise location of each vehicle within the study area every one-tenth of a second, resulting in detailed lane positions and locations relative to other vehicles.

We first uploaded the vehicles trajectory data given in the data sets into the MATLAB R2023 workspace. Then, we proceeded using MATLAB's Signal Processing Toolbox, that provides advanced filtering and smoothing techniques that can help remove noise from the raw trajectory data. This is crucial for accurate calculation of variables like speed and acceleration, which are sensitive to small positional errors. We calculated the average space headway, time headway, speed, and flow for each second of the 15 minutes and plotting the curves. Next, we used the MATLAB R2023 fitting curve tool to get an approximation of the mathematical function of the studied variables and extract their frequencies and investigate their values. The fitting curve tool in MATLAB, beyond just approximating mathematical functions, allows for the exploration of different model types (e.g., polynomial, exponential, Fourier series) to best represent the observed data. This flexibility can reveal underlying patterns in traffic behavior that might not be apparent from simple visualization of the raw data.

For confirmation, the HighD German database is also used [21]. Unlike the NGSIM data, which was collected in 2005, the HighD data is more recent, with recordings made between 2017 and 2018. This allows for comparison of traffic patterns over time. The HighD dataset provides naturalistic vehicle trajectories recorded on German highways using a drone. The use of drones for data collection provides a wider field of view and potentially less disruption to normal traffic flow compared to stationary cameras. Traffic was recorded at six different locations and the sections were 420 meters long. Each vehicle's trajectory, including vehicle type, size, and maneuvers, is automatically extracted into a detailed CSV file.

For further validation of our findings from the NGSIM data, we applied the same empirical analysis method to the HighD dataset. The vehicle trajectory information from the HighD CSV files was imported into the MATLAB R2023 workspace. Following the established procedure, we utilized identical signal treatment tools to calculate the average space headway, time headway, speed, and flow for each second of the recorded periods. As with the NGSIM data, we visualized these results through curve plotting. Maintaining methodological consistency, we employed the MATLAB R2023 fitting curve tool to approximate mathematical functions for the studied variables, extract their frequencies, and investigate their values. This parallel analysis of the HighD data served to confirm the patterns and relationships observed in the NGSIM datasets.

2.2. Cellular Automata

Cellular automata (CA) are discrete models consisting of a grid of cells with finite states that evolve based on simple rules and neighboring states. In traffic modeling, CA are valued for their ability to simulate complex traffic behaviors from simple local interactions [22]. They offer computational efficiency, scalability, and can reproduce emergent phenomena like traffic jams. CA's discrete nature in both space and time makes them ideal for large-scale simulations and real-time applications. Their rule-based approach allows easy incorporation of various traffic scenarios and driver behaviors. While sacrificing some detail, CA provide a balance between simplicity and realism, making them crucial in traffic flow theory and urban planning [23]. In addition to all that, CA models have the ability to reproduce phase transitions in traffic flow, which can guide us to capture complex macroscopic phenomena from microscopic interactions. The Nagel-Schreckenberg (NaSch) model is a popular cellular automaton approach for traffic flow simulations. Introduced in 1992, it uses simple rules to represent vehicle movement on a discretized road. Despite its simplicity, the NaSch model effectively captures key traffic phenomena like spontaneous jam formation and stop-and-go waves. For these reasons, we chose to adopt this model. The NaSch computational model is defined on a one-dimensional array of L sites and with periodic boundary and open boundary conditions. Each site can either be occupied by a single vehicle or remain empty. Each vehicle has an integer velocity ranging from zero to Vmax. For any given configuration, the system is updated in four consecutive steps, performed simultaneously for all vehicles [24]:

I) Acceleration: if the velocity v of a vehicle is lower than Vmax and if the distance to the next car ahead is larger than $v + 1$, the speed is advanced by one $[v \rightarrow v + 1]$.

2) Slowing down (due to other cars): if a vehicle at site i sees the next vehicle at site $i + j$ (with $j \leq v$), it reduces its speed to $j-1$ $[v \rightarrow j-1]$.

Journal of Theoretical and Applied Information Technology
15th November 2025. Vol.103. No.21

ISSN: 1992-8645 www.jatit.org E-ISSN: 1817-3195

3) Randomization: with probability p, the velocity of each vehicle (if greater than zero) is decreased by one [v → v-1].

4) Car motion: each vehicle is advanced v sites.

2.2.1. Periodic boundaries:

It implies that the road is dealt with as a continuous loop in order to conserve the total number of vehicles (closed loop as in car races) [22]. When a vehicle moves past the last cell, it reappears at the first cell, maintaining a consistent vehicle density across the simulation. We set the value of the array sites at L=1000 cells and periodic boundaries, for Vmax=1 to 5, we run the program for 10000-time iteration for the different states of traffic density (free flow, critical density, and jam) in the deterministic case (null braking probability P=0). We extracted and plotted the following variables: space headway, time headway, speed. We repeated the same procedure for the non-deterministic case (P≠0).

2.2.2. Open boundaries:

The open boundary conditions allow vehicles to enter and exit the road. This setup is more representative of real-world traffic scenarios compared to periodic boundaries, which assume a closed-loop system [24]. By adjusting the injection (α) and extraction (β) rates, researchers can simulate various traffic conditions, from free flow to congested states. Hence, the open boundaries are implemented by defining an injection and extraction strategies:

- The expended injection strategy where we create a mini system with Vmax+1 cells length at the beginning of the system. At each iteration, with a probability α, a new vehicle is introduced with a speed equal to Vmax and is positioned at a distance equal to Vmax to the first vehicle in the road [25].

- The extraction strategy: when the leading vehicles arrive to the right boundary of the cell chain (the end of the chain) they exit with the probability.

N.B: since the time is discretized, probability and rate refer to the same meaning.

2.3. Empirical Formulations of Demand and Discharge Rates:

In the empirical analysis, the injection parameter α, also called demand rate, corresponds to the probability of having a vehicle aiming to enter the road also known as the demand. The demand represents the number of vehicles arriving to the entry of a specific facility desiring to use it. We calculate it using the following formula: $\alpha = q_{in}/q_{max}$,with q_{in} the effective inflow and q_{max} is the maximum flow entering the section. Similarly, the extraction rate β, also named as discharge rate, corresponds to the volume of vehicles discharging and is inversely proportional to the service time. It is calculated using the following formula: $\beta = q_{out}/q_{max}$, with q_{out} is the effective outflow and q_{max} is the maximum flow exiting the section.

Finally, we utilized both the periodic and the open boundaries models because they have different aims ang goals. The open boundaries is used since it can approach the realistic highway traffic scenarios while the periodic boundaries are useful for studying intrinsic traffic dynamics.

3. RESULTS AND DISCUSSIONS:

In this section, we will display in detail the empirical results and the reproduced traffic phenomenon in the NaSch periodic and open boundaries.

3.1. Empirical Results:

At first, we extracted the data from each file of the two used datasets and uploaded them into the MATLAB R2023 and plotted the following variables over time: vehicles average speed, time headway and space headway. For space management, we only kept the I-80 recording from 5:15 to 5:30 (Fig.1). We observed from these figures that the plotted variables exhibit a periodic behavior. We proceeded then to identify the phase traffic of each time recording.

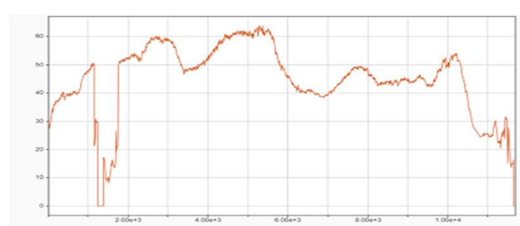

(a)

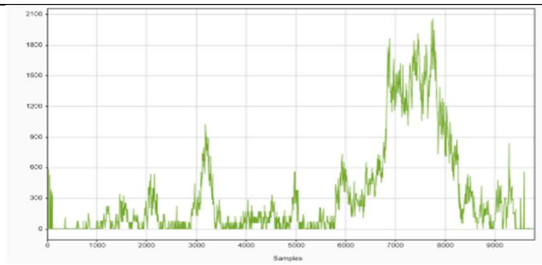

(b)

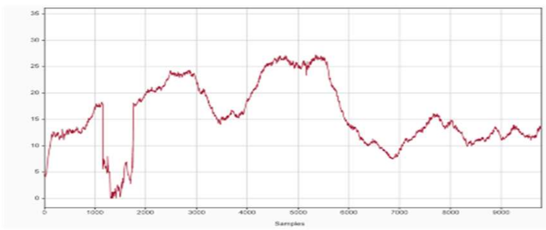

(c)

Figure 1: For I-80 From 5:15 to 5:30(a) Space Headway(b) Time Headway (c) Speed

3.1.1. Investigation of traffic phases:

Traffic flow exhibits distinct phases. While more complex phases distinction exists, a simplified model consisting of free flow, congestion, and jam phases is often adopted for its clarity and practicality. This simplified model, while not capturing all the nuances of traffic dynamics, provides a useful framework for understanding and analyzing traffic behavior in various contexts, from urban planning to traffic control systems [16]. In the following sections, we will be adopting this model since our objective is to only define the traffic phase of each studied section.

The first method we used was by calculating the index of congestion using the following formula Eq. (1):

$$I = \frac{\text{free flow travel time}}{\text{measured travel time}} \quad (1)$$

If the value of the index of congestion obtained is close or equal to 1 this means that it is the free flow, if it is lower than 1 and great or equal than 0.5 so the traffic is low congested, else if it is lower than 0.5 than the traffic is highly congested.

Table 1: The Index of Congestion of Different Recordings.

I-80	4:00 TO 4:15	5:00 TO 5:15	5:15 TO 5:30
Index of congestion	0.0194	0.0326	0.0148
US-101	7:50 to 8:05	8:05 to 8:20	8:20 to 8:35
Index of congestion	0.0597	0.0458	0.0619
HighD recording	03	25	26
Index of congestion	0.97	0.28	0.52

The calculations of the index of congestion are displayed in the table1. For the I-80 and US-101 locations, the index of congestion values are below 0.5 and close to 0, so all the recording are in the jamming traffic state. But in the HighD datasets, the recording number 03 is in the free flow state because the value of the index of congestion is close to 1, the recordings number 25, we are in the jamming state of traffic because the value of the index is below 0.5. and last the recording 26, the index of congestion is between 0.5 and 1, we conclude that we are in the congestion.

For the HighD data base, based in the index of congestion and from comparing the mean speed to the max speed as shown in the table (table2) we can say the phase separation can be done easily, the recording 3 represents the free flow, the recording 25 represents the jam and the recording number 26 is the congestion.

Table2: The Maximum Velocity and The Average Velocity of HighD Studied Recordings.

Recording number	03	25	26
Vmax(m/s)	33.33	33.33	33.33
Vmean(m/s)	31.74	10.31	19.04

This approach cannot hold for the NGSIM data base. Indeed, for more specific phase separation of the NGSIM data base I-80 and US-101 recordings, we opted for the cross-correlation between flow and density [26]. The flow and density cross-correlation is positive for the free flow, it is equal to zero in the congestion and negative if we are in the jamming phase. As for the studied data we obtained the results in table 3.

Table3: The Cross- Correlation Coefficient of the I-80 And US-101 Sections

I-80	4:00 TO 4:15	5:00 TO 5:15	5:15 TO 5:30
Frequency	8.71×10^{-2}	2.23×10^{-4}	2.651×10^{-2}
US-101	7:50 TO 8:05	8:05 TO 8:20	8:20 TO 8:35
Frequency	1.58×10^{-2}	3.92×10^{-4}	2.25×10^{-4}
HighD recording n°	03	25	26
Frequency	0.2423	0.0067	0.0045

I-80	4:00 TO 4:15	5:00 TO 5:15	5:15 TO 5:30
Cross - correlation	-0.9028	-0.5632	-0.9512
US-101	7:50 TO 8:05	8:05 TO 8:20	8:20 TO 8:35
Cross correlation	- 0.9476	-0.3593	- 0.3034

From the results (table3), for the I-80 section we can say for the time intervals from 4:00 to 4:15 and from 5:15 TO 5:30 the cross-correlation coefficient is negative and close to -1, we can say that we are in the jamming phase, and for the remaining 15 minutes from 5:00 to 5:15 the cross-correlation coefficient is negative also and close to 0 so we are in the congestion.

Similarly, for the US-101 section, for the first 15 minutes from 7:50 to 8:05 the coefficient is negative and close to-1 that means we are in the jam. For the remaining 30 minutes, from 8:05 to 8:20 and from 8:20 to 8:35 the coefficient is negative and close to zero hence we are in the congestion traffic phase.

3.1.2. Angular frequency and period extraction

In the following step, we uploaded the values of the previously selected variables in the curve fitting tool of MATLAB R2023 to extract the angular frequency of each recording and found the function that fits the best these sets of data. We obtained the results displayed in the table4. The curve fitting reveals that these oscillations are a sum of sines and cosines, more precisely an eight-degree Fourier Serie that can be written as follows:

$$s(t) = a_0 + \sum_{n=1}^{8} (a_n \, cos(\, n.w.t) + b_n \, sin(n.w.t)) \quad (2)$$

Or

$$s(t) = a0 + a1.cos(w.t) + b1 * sin(w.t) + a2.cos(2.w.t) + b2.sin(2.w.t) + a3.cos(3.w.t) + b3.sin(3.w.t) + a4.cos(4.w.t) + b4.sin(4.w.t) + a5.cos(5.w.t) + b5.sin(5.w.t) + a6.cos(6.w.t) + b6.sin(6.w.t) + a7.cos(7.w.t) + b7.sin(7.w.t) + a8.cos(8.w.t) + b8.sin(8.w.t). \quad (3)$$

With ω is the angular frequency and a_n and b_n constants.

Table4: The Angular Frequency of The Traffic Variables Obtained by The Curve Fitting Tool.

After investigating the angular frequency values, we obtained that for the I-80 first and last recordings (from 4:00 to 4:15 and from 5:15 to 5:30), the US-101 first recoding from 7:50 to 8:05 the 3rd and 25th HighD recordings, in both the jamming phase and the free flow, that the angular frequency is a function of a time variable, that we can define as the period of the jamming phase and free flow, and it can be defined as follow:

$$w = 2\pi/T \quad (4)$$

And for the I-80 recording from 5:00 to 5:15, the US-101 second and last recordings from 8:05 to 8:20 and from 8:20 to 8:35 and the 26th HighD recording, the congestion phase, the angular frequency is the inverse of another time variable:

$$w = 1/T \quad (5)$$

Journal of Theoretical and Applied Information Technology
15th November 2025. Vol.103. No.21

ISSN: 1992-8645 www.jatit.org E-ISSN: 1817-3195

Hence, we obtain the period values in table5.

Table5.The Period of The Traffic Variables.

I-80 recording time	4:00 TO 4:15	5:00 TO 5:15	5:15 TO 5:30
Period (s)	721.376	4484.30	237.011
US-101recording time	7:50 TO 8:05	8:05 TO 8:20	8:20 TO 8:35
Period(s)	397.660	2551.02	4444.44
HighD recording n°	03	25	26
Period (s)	25.93	937.78	222.22

The traffic flow dynamics, especially under congested conditions, exhibit oscillatory patterns that closely resemble those of coupled harmonic oscillators. Researchers have explored this analogy to gain valuable insights into traffic behavior. In this context, several key similarities emerge, including angular frequency and period, they are fundamental concepts that apply to both harmonic oscillators and traffic oscillations, describing the rhythmic nature of these systems. In harmonic oscillators, angular frequency represents the number of oscillations per unit time, while in traffic, it describes the rate of stop-and-go cycles at a fixed point [16,27]. Period, being the inverse of frequency, denotes the time for one complete oscillation or traffic wave [28,16]. Mathematical modeling of car-following behavior can resemble the equations for harmonic oscillators. Wagner (2011) proposed a time-discrete harmonic oscillator model. Concepts of angular frequency (rate of oscillation) and period (time between successive waves) are applicable to both systems, although more complex in traffic systems [16]. In multi-vehicle traffic flow, the behavior of each vehicle influences and is influenced by neighboring vehicles, similar to coupled oscillators [28,35]. By analogy, we acquired that in the case of the I-80 first and last recordings (from 4:00 to 4:15 and from 5:15 to 5:30), the US-101 first recoding from 7:50 to 8:05 the 3rd and 25th HighD recordings, in both the jamming phase and the free flow, the period is the average travel time of the vehicles T_0. And in the case of the I-80 recording from 5:00 to 5:15, the US-101 second and last recordings from 8:05 to 8:20 and from 8:20 to 8:35 and the 26th HighD recording, the congestion phase, the period is expressed as ,with τ the relaxation time , it is the time that a driver requires to perceive and process the traffic conditions and adjust the vehicle speed according to these conditions [29] it can be expressed as

$$\tau = \int t.v(t)\,dt / \int v(t)\,dt \quad (6)$$

With t the time in seconds and v the average speed at the time t [30].

3.2. Summary

To sum up the empirical results, we found that the traffic oscillations are persisting regardless of the traffic phase and that the traffic variables exhibit a periodic behavior, its function is an eighth Fourier series (Eq. (2), Eq. (3)) for which the period of these traffic variables in the free flow and the jam is the vehicles average travel time T_0 and, in the congestion, is the relaxation time τ. It was also found that no matter the type of the road section (with or without on-ramp and off-ramp), the oscillations are persistent. The analogy between traffic flow dynamics and coupled harmonic oscillators provides a valuable framework for understanding and modeling complex traffic behaviors, allowing us to apply mathematical concepts from physics to analyze traffic oscillations period and frequency.

3.3. Simulations Results:

For further understanding of the phenomenon of oscillations, we choose to reproduce them in the simulations using the NaSch model, check the results found in the previous section and go beyond that.

3.3.1. Nasch with periodic boundaries:

In this section of our study, we proceeded with a L=1000 cells chain with a randomly distributed number of vehicles depending on the density, a maximum velocity Vmax varying between 1 and 5 and then we collect the space headway, time headway, flow, and speed at each iteration.

3.3.1.1. The free flow

For the deterministic case (P=0), for different Vmax, we set the value of the density in the interval $[0.01, 1/Vmax + 1[$, we exhibit a periodic behavior with a repeated pattern as seen in Fig. 2. The fitting of these curves shows that the studied variables are sine and cosine functions (eighth degree Fourier series) (Eq. (2), Eq. (3)). For the maximum speed Vmax=3 and Vmax=5, we extracted the angular frequency of the studied variables in the density free flow interval (table 6 and table 7). Our calculations of the theoretical angular frequency closely matched the experimentally extracted values, corroborating our previous findings. Analysis of the data presented in Tables 6 and 7 reveals a significant insight: the angular frequency in the free flow regime appears to be solely dependent on the maximum speed. This observation suggests that other parameters, such as fluid density, do not significantly influence the angular frequency under these conditions. This relationship between maximum speed and angular frequency not only validates our initial hypotheses but also provides a simplified framework for understanding the dynamics of free flow systems.

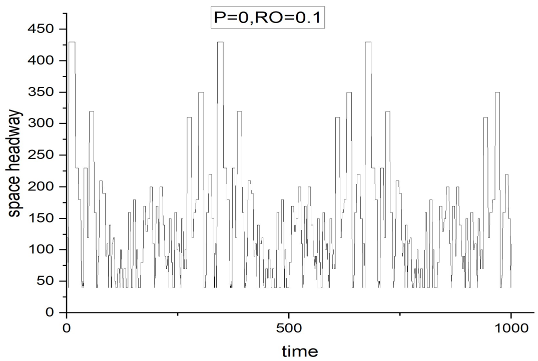

(a)

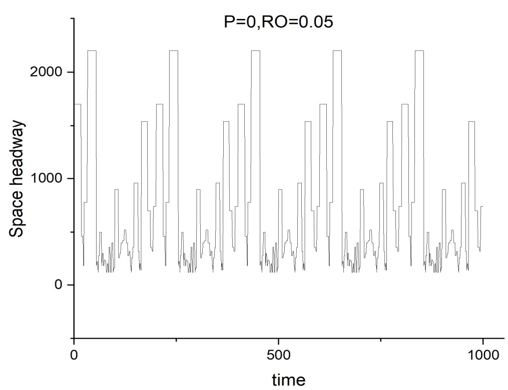

(b)

Figure 2: Space Headway (a) Vmax=3 And (b) Vmax=5

We repeated the same step for the non-deterministic case (P≠0), the graphs revealed a periodic behavior but without a repeated pattern as follows (Fig. 3). The function of the parameters in this case is also an eight Fourier Serie (equation2,3) with the same angular frequency ($w = 2\pi/T_0$).

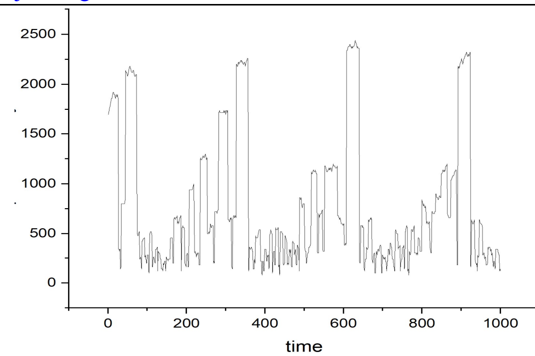

Figure 3: Space Headway Vmax=4 P=0.1

3.3.1.2. The congestion:

For the deterministic case, we set the value of the density at the critical density ($Kc = 1/Vmax + 1$) ,the curves behavior become a pseudo-periodic behavior for the different values of Vmax as seen in Fig. 4. The curve fitting of all variables displays that it is a sine and cosine as well (Eq. (2), Eq. (3)). To validate the empirical findings, first, we calculated the relaxation time using Eq. (6). Subsequently, we used this value to determine the corresponding angular frequency through Eq. (5). We then compared this theoretically derived angular frequency with the obtained value from the curve fitting tool. The results showed a remarkable concordance between the theoretical predictions and the obtained values.

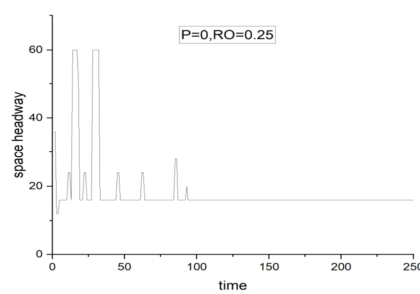

(a)

ISSN: 1992-8645 www.jatit.org E-ISSN: 1817-3195

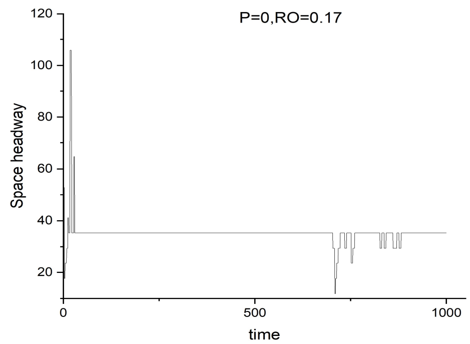

(b)

Figure 4. Space Headway (a) Vmax=3 And (b) Vmax=5

In contrast to the deterministic scenario, the non-deterministic case of this traffic phase exhibits persistent oscillations. These oscillations maintain a consistent angular frequency, which is inversely proportional to the relaxation time. We calculated this relaxation time and subsequently confirmed that its inverse indeed matches the observed angular frequency, as predicted by Eq. (5). This behavior is clearly illustrated in Fig. 5, highlighting the sustained nature of these oscillations in the non-deterministic traffic flow.

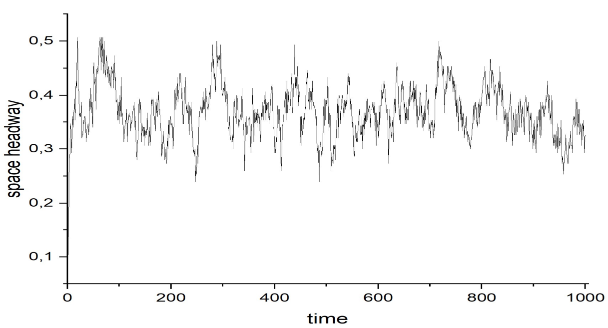

Figure 5: Space Headway Vmax=4 P=0.5 K=0.8

3.3.1.3. The jam

In the case of the jamming phase, it emerges when the traffic density exceeds the critical density. for different values of Vmax, the periodic behavior reappears but with no repeated pattern as observed in the Fig. 6. The curve fitting gives that the studied variables are sine and cosine functions (eighth degree Fourier series) (Eq. (2), Eq. (3)). And by calculation the average vehicle travel time and comparing it to the extracted value of frequency, we confirmed that the angular frequency of this variables in this case is $w = 2\pi/T_0$, with T_0 the average travel time.

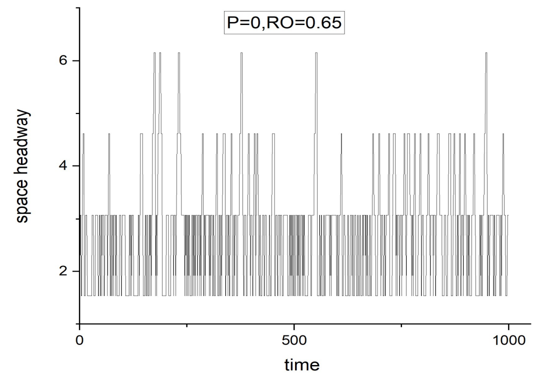

(a)

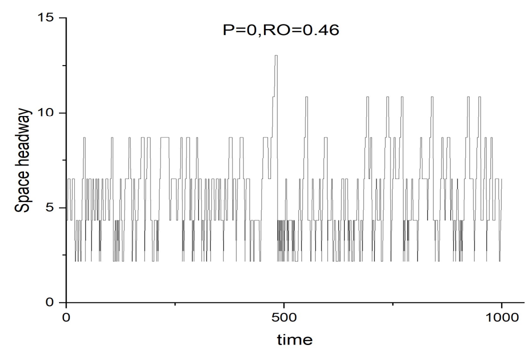

(b)

Figure 6: Space Headway(a) Vmax=3 and (b) Vmax=5

For the maximum speed Vmax from 1 to 5, we extracted the angular frequency of the studied variables in the density free flow interval and obtained the results displayed in table8. The table(table8) reveals an intriguing pattern regarding the relationship between maximum velocity and angular frequency. Specifically, for any given maximum velocity, the corresponding angular frequency value remains constant, irrespective of changes in density. This consistency suggests that, within the jamming phase, the frequency is primarily determined by the maximum velocity and appears to be independent of density variations.

Table8: The Angular Frequency for Different Values of Vmax and Densities.

Vmax	0.7	0.8	0.9
1	0.0004	0.0004	0.0004
2	0.0107	0.0107	0.0103

ISSN: 1992-8645 www.jatit.org E-ISSN: 1817-3195

3	0.0109	0.0109	0.0102
4	0.0109	0.0109	0.0102
5	0.0109	0.0109	0.0102

As for the non-deterministic case, the periodic behavior persists (Fig.7). We proceeded with the same steps, and we extracted ed the frequencies. This analysis reveals a persistent oscillatory behavior in the traffic flow, even under congested conditions. Notably, we discovered that the period of these oscillations corresponds precisely to the average travel time of vehicles in the system. This finding aligns remarkably well with our empirical observations.

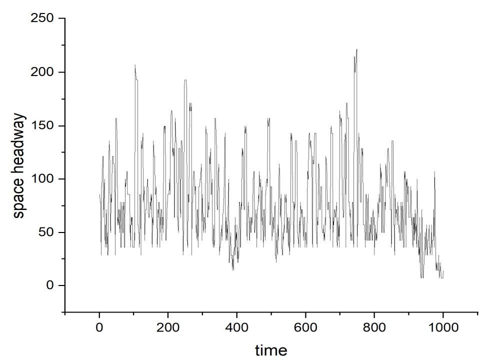

Figure 7: Space Headway Vmax=4 And P=0.25 And K=0.7.

3.3.2. Nasch open boundaries:

We ran the simulations with considering a single lane road of L=500 cells chain with the maximum speed varying from 1 to 5 for both the deterministic and non-deterministic cases.

3.3.2.1. The deterministic case(P=0):

In this case, we plotted the vehicles average speed, and we observe the persistence of the periodic behavior as we can see in the Fig. 8, Fig. 9 and Fig. 10. In these figures (Fig.8, Fig. 9, Fig. 10), we can observe the relationship between vehicle speed and different traffic phases, clearly illustrating the transitions between traffic phases. The graphs demonstrate how speed varies across the free flow, congested and jamming phases of traffic. In the free flow phase, we see consistently high speeds vehicles. As we transition into the congested phase, there is a noticeable decrease in speed, though traffic. The transition to the jam phase is marked by a sharp drop in speed, often approaching zero. Next, we used the MATLAB R2023 curve fitting tool and we were able to obtain the angular frequency of all the variables for all the couples' injection rate α and extraction rate β, for the entire range of Vmax from 1 to 5, in the table9. It is worth to mention, that this table do not vary when varying Vmax, thus, for simplification purposes, we will only focus on the case of Vmax=5.We can observe that for the injection rate α lower than the extraction rate β and for the injection rate α is greater than the extraction rate β the angular frequency of the variables is equal to $w=2\pi/T_0$, but for the case where the injection rate α is equal to the extraction rate β the frequency is inverse of the relaxation time τ.

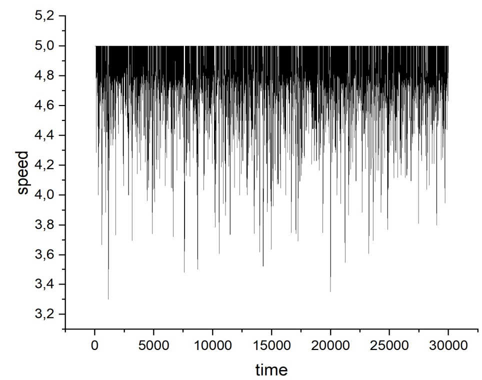

Figure 8: speed for Vmax=5 α=0.2 and β=0.4

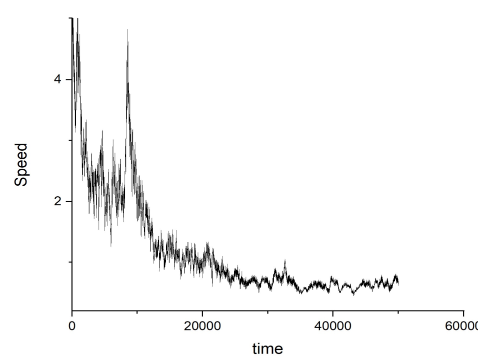

Figure 9: speed for Vmax=5 α=0.4 β=0.4

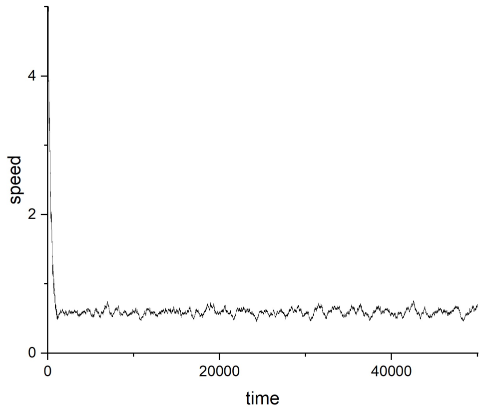

Figure 10: Speed For Vmax=5 A=0.6 B=0.4

Next, we plotted the phase diagram for L=500 cells, Vmax=5 and P=0 (Fig. 11). In the Fig.11, the red line represents the boundary between free flow and jammed states, representing the critical point where traffic congestion begins to form. Hence, the period of these points is T=2πτ, with τ is the relaxation time.

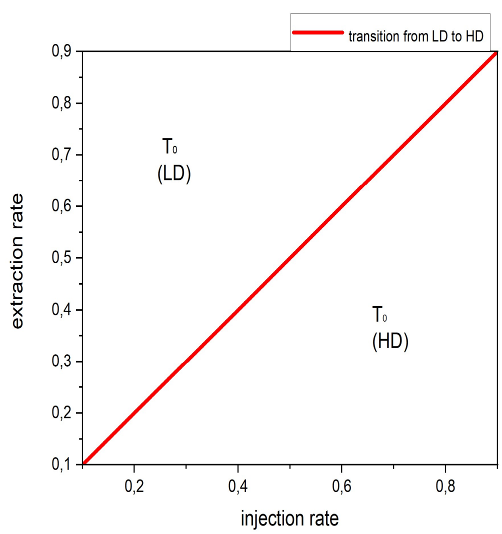

Figure 11: Phase Diagram for Vmax=5 and P=0.

3.3.2.2. The non-deterministic case (P≠0):

In the proceeding step, we kept the same simulation parameters except for the breaking probability that was set to P=0.5 and when we plotted the average speed of vehicles, for Vmax=5, the oscillations also persisted as we can observe in the graphs (Fig. 12 and Fig. 13 and Fig. 14). The figures (Fig. 12, Fig. 13 and Fig. 14) illustrate the relationship between vehicle speed and various traffic phases, clearly showing the transitions between these phases. These graphs depict how speed changes across three distinct traffic states: free flow, congested, and jamming phases. In the free flow phase, vehicles maintain consistently high speeds with minimal interference. As traffic transitions into the congested phase, we observe a notable reduction in speed, although vehicles continue to move. The shift to the jam phase is characterized by a dramatic decrease in speed, with traffic often slowing to a near standstill. These visualizations provide valuable insights into the dynamic nature of traffic flow and the critical points at which traffic behavior significantly changes. After that we used the curve fitting tool, we were able to obtain the angular frequency of all the variables for all the couples α and β in the table 10.

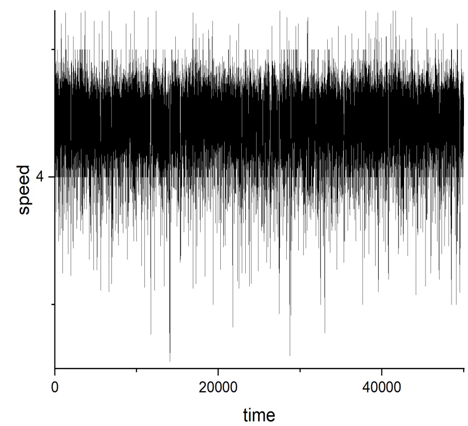

Figure 12: Speed For Vmax=5 α=0.12 β=0.5 and p=0.5.

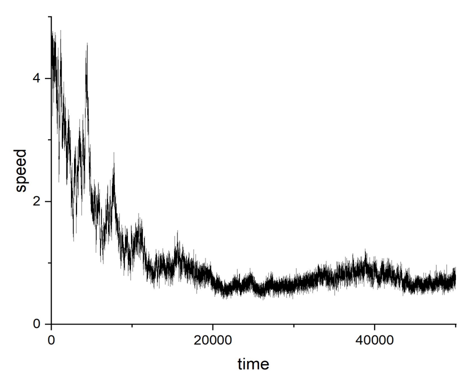

Figure 13: Speed for Vmax=5 α=0.25 β=0.5 and P=0.5.

Journal of Theoretical and Applied Information Technology
15th November 2025. Vol.103. No.21

ISSN: 1992-8645 www.jatit.org E-ISSN: 1817-3195

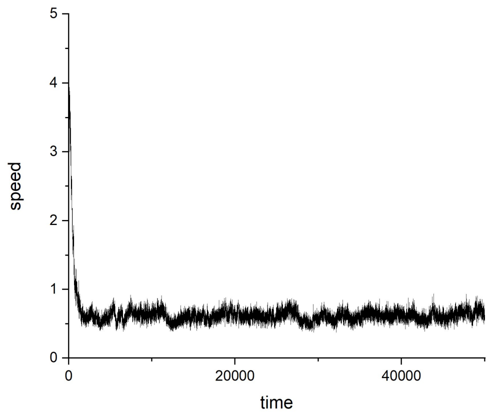

Figure 14: Speed for Vmax=5 α=0.8 β=0.5 and P=0.

Next, we plotted the phase diagram for L=500 cells, Vmax=5 and P=0.5 and obtained the Fig. 15. Similarly, in the non-deterministic case, the red line indicates the transition between free flow and congested traffic. At this critical boundary, the system exhibits oscillations with a period T = 2πτ, where τ is the relaxation time.

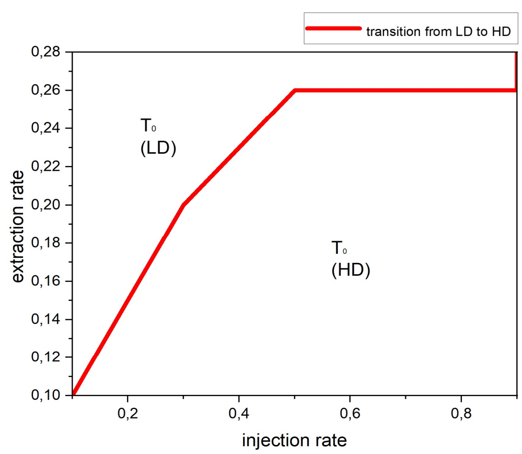

Figure 15: Phase Diagram for Vmax=5 and P=0.5.

In this step, we calculated the injection rate α and the extraction rate β for a 5-minute time interval of the I-80 and US-101 locations data set and associated each (α, β) couple with its obtained angular frequency and its corresponding traffic phase, and we obtained the table 11. The empirical analysis focused on road sections that closely resemble the open boundary conditions of the non-deterministic NaSch model. We conducted a comparative study between our empirical results and the model's predictions, specifically examining the injection rate α, extraction rate β, and their corresponding traffic phases. Our findings corroborated the model's predictions. It is important to note that this approach is qualitative rather than quantitative, providing insights into general patterns and behaviors rather than precise numerical predictions.

3.4. Summary

In this section, our primary aim was to transcend the limitations of purely empirical observations, therefore we used the Nasch model, known for its ability to capture complex traffic dynamics, provided a robust platform to test our hypothesis across a wide range of simulated traffic conditions. We proved that the oscillations persist through the different traffic phases and states, and can be written as a sum of sines and cosines, then we proceeded to confirm the period and the angular frequency formulas found previously for the different traffic states in both cases deterministic and non-deterministic and for both periodic and open boundaries of the NaSch model:

a) Free flow

In this case the period is the average vehicles travel time T_0. Hence, the angular frequency of the studied traffic variables is $w = 2\pi/T_0$. It was noticed that the angular frequency in the case of free flow depends only on Vmax.

b) Congestion

For the congested phase, the period is $2\pi\tau$ with τ being the relaxation time. Hence, the angular frequency of the studied traffic variables obtained in the beginning of this section is proved to be $w = 1/\tau$.

c) Jam

For the jamming phase, case the period is the average vehicles travel time T_0. Hence, the angular frequency of the studied traffic variables is $w = 2\pi/T_0$. In this case the angular frequency depends only on the traffic density.

These findings align remarkably well with our empirical observations, providing a robust connection between theoretical predictions and real-world traffic dynamics. The consistency between the oscillation period and the average travel time suggests a fundamental relationship in traffic flow, where the rhythmic patterns of vehicle movement are intrinsically linked to the time vehicles spend traversing the observed area. This insight not only

ISSN: 1992-8645 www.jatit.org E-ISSN: 1817-3195

validates our theoretical framework but also offers a practical metric for understanding and potentially predicting traffic behavior in congested scenarios.

4. INVESTIGATING TRAVEL TIME AS A MEASUREMENT METRIC:

The vehicles travel time serve as a crucial metric in traffic analysis, providing valuable insights into the efficiency and performance of road networks. This measurement represents the duration a vehicle spends traversing a specific route or segment of roadway. By tracking travel times, traffic engineers and planners can assess the level of congestion, identify bottlenecks, and evaluate the effectiveness of traffic management strategies. In the previous section we proved that the traffic oscillations period at jamming and free flow phases is the vehicles average travel time T_0, in this section we will investigate its importance as a characteristic time.

Firstly, we calculated the average mean speed and space head way in the available multiples of the travel time for the previously studied sections: I-80 from 5:15 to 5:30 and the US-101 from 7:50 to 8:05. After analyzing the data (table 12,13 and 14), interestingly, the results showed remarkable consistency with measurements obtained using travel time as the basis, with one notable exception, the I-80 third recording. This striking similarity in values leads to an intriguing hypothesis: we may be able to use travel time as the measurement time instead of arbitrarily chosen durations. This approach could potentially offer a more standardized and meaningful basis for traffic flow analysis. The consistency observed in most cases suggests that travel time might serve as a natural, characteristic time scale for traffic measurements. However, to rigorously test and confirm this hypothesis, we employ simulations using NaSch model. Then, we calculated the average mean speed and space head way in the available multiples of the travel time for periodic boundaries for both deterministic and non-deterministic cases in the jamming phase($K=0.7$) and $V_{max}=5$ and obtained the results displayed in tables 15 and 16.

To validate our hypothesis regarding the use of travel time as a measurement time, we conducted extensive simulations using the Nash model. These simulations corroborated our initial findings from the empirical data analysis, with an important condition: the results hold true under the condition that traffic is stable and homogeneous. Under stable and homogeneous traffic conditions, the results of these simulations strongly supported our earlier observations: using travel time as the measurement time yielded results consistent with those obtained using traditional fixed-duration measurements. This consistency held true for key traffic parameters such as average speed and space headway. The simulations also helped us understand the conditions under which the single observed discrepancy in our empirical data might occur, particularly when traffic stability or homogeneity was compromised. These comprehensive simulation results bolster our confidence in proposing travel time as a viable and potentially superior alternative to arbitrary measurement durations in traffic flow analysis, specifically for stable and homogeneous traffic conditions.

5. CONCLUSION:

Traffic oscillations, represent a significant challenge, particularly in congested conditions. While some researchers proved that these oscillations are a result of the human behavior, others suggested that system instability, phantom jams and merging and diverging flows are the main causes of traffic oscillations. Despite extensive research, the precise equation for the period and the angular frequency of these oscillations remains elusive. In this paper, we have uncovered new insights and addressed critical questions that had previously remained unanswered.

We followed the empirical studies path, for separate locations in different countries, and we discovered that the oscillations are persistent no matter the value of the traffic density (high or low). In addition to that, we concluded that the oscillations persist no matter the type of the road section: the presence and/or the absence of on ramps and off ramps. This indicates that the traffic oscillations are a universal phenomenon that occurs independently of both traffic density and road design. On top of that, we extracted the equation of microscopic and macroscopic traffic variables (average speed, time headway and space headway), we determined that it is a sum of sines and cosines, more precisely an eight-degree Fourier Serie. This mathematical characterization suggests that the traffic can be analyzed and modeled using harmonic components. In this context, we discussed that traffic flow dynamics, especially under congested conditions, exhibit oscillatory patterns that closely resemble those of coupled harmonic oscillators. Also, researchers have explored this analogy to gain valuable insights into traffic behavior. Hence, this finding can confirm that we can modelize traffic as a system of coupled oscillators, where each vehicle is viewed as an oscillator, with its position and velocity represent its state. By analogy, we were able to dig up the formula of the oscillation's period and frequency. In case of the free flow and jam, the period is the average vehicles travel time T_0. Accordingly, the angular frequency can be expressed as follows $w = 2\pi/T_0$ .While in the case of the congested traffic, the period the period is $2\pi\tau$ with τ being the relaxation time. Accordingly, the angular frequency is the inverse of the relaxation time τ.

To confirm these conclusions and go beyond, we opted for an investigation of oscillations based on Cellular Automata using the NaSch model, adopting both periodic and open boundaries, in the deterministic and non-deterministic cases. The simulations results revealed that traffic oscillations persisted across all traffic states, in both scenarios. The presence of traffic oscillations in case of the non-deterministic case, null braking probability, strengthens the presence of the oscillations in all the traffic states, despite the human impact, it also emphasizes their significance in understanding and modeling traffic dynamics, as they appear to be an intrinsic feature of vehicular flow rather than a result of particular circumstances such as congestion or modeling assumptions. Indeed, we were not only able to verify the period and the angular frequency formula but also, we found that in the free flow the angular frequency depends only on the value of the maximum velocity while, in the jamming phase, the angular frequency depends only on the value of the density, in both the deterministic and non-deterministic conditions.

In the context of applying our findings on traffic oscillation frequency and period, our comprehensive investigation into traffic flow measurement methodologies yielded significant results. The research provides compelling evidence supporting the use of vehicle travel time as a fundamental measurement metric. Initially, we analyzed empirical data from three diverse locations across two countries, focusing on key traffic parameters such as average speed and space headway. This real-world data revealed a striking correlation between measurements based on travel time and those derived from traditional fixed-duration sampling methods. To rigorously test and validate these empirical findings, we employed the NaSch model simulations. These simulations not only corroborated our initial observations but also provided insights into the conditions under which travel time-based measurements are most effective. Specifically, we found that the consistency and reliability of this approach are highest in stable and homogeneous traffic conditions.

The strong agreement between real-world observations and theoretical models strengthens our hypothesis that travel time can serve as a more natural and meaningful measurement time scale in traffic studies. This approach offers several potential advantages over traditional fixed-duration measurements. Firstly, it inherently captures the dynamic nature of vehicular movement, providing a more context-aware representation of traffic flow. Secondly, it offers the possibility of standardizing traffic analysis across different road configurations and traffic states, potentially improving the comparability of studies conducted in diverse environments.

The quantification of the frequency and period of traffic oscillations represents a significant advancement in our understanding of traffic dynamics. These findings provide an insight into the rhythmic nature of congestion patterns. By identifying the temporal characteristics of these oscillations, traffic engineers and urban planners can now develop more targeted interventions to diminish the impact of these oscillations. For instance, ramp metering and adaptive traffic signal systems could be regulated to compensate the oscillation frequencies, by potentially dampening their effects. Furthermore, this knowledge could inform the design of autonomous vehicle algorithms, allowing them to anticipate and mitigate oscillations more effectively. On a broader scale, these findings contribute to the development of more accurate traffic prediction models, enabling better real-time traffic management and long-term infrastructure planning. Ultimately, this research paves the way for innovative solutions that could significantly reduce congestion, improve fuel efficiency, and enhance overall road safety.

To sum up, this based on real-world traffic data study has provided valuable insights into the period and the angular frequency of the traffic oscillations and lead us to reveal that they occur regardless of the traffic phase, the type of road section or the types of drivers and their period and angular frequency varies depending on the traffic state. In other words, the traffic oscillations are a universal intrinsic phenomenon since the fluctuations of the microscopic and macroscopic variables persists throughout the different traffic conditions. However, this study is only a preliminary step toward understanding and mitigating these oscillations. A comprehensive investigation requires a multifaceted

ISSN: 1992-8645 www.jatit.org E-ISSN: 1817-3195

approach that combines empirical observations and advanced modeling techniques.

While this study establishes new insights into the intrinsic nature of traffic oscillations, certain limitations should be acknowledged. This work focuses primarily on freeway traffic under continuous flow conditions, which may not capture the complexity of urban or mixed traffic environments. Second, the NaSch cellular automaton model analysis was restricted to homogeneous traffic without lane-changing, which simplifies real driving .Future work will expand the analysis to cover more traffic scenarios and incorporate more detailed behaviors.

REFERENCES:

[1] Herty, M., and R. Illner. 2008. "On Stop-and-Go Waves in Dense Traffic." Kinetic & Related Models 1 (3): 437-452. https://doi.org/10.3934/krm.2008.1.437.

[2] Laval, J. A., and L. Leclercq. 2010. "A Mechanism to Describe the Formation and Propagation of Stop-and-Go Waves in Congested Freeway Traffic." Philosophical Transactions of the Royal Society A: Mathematical, Physical and Engineering Sciences 368 (1928): 4519-4541. https://doi.org/10.1098/rsta.2010.0138.

[3] Portz, A., and A. Seyfried. 2011. "Analyzing Stop-and-Go Waves by Experiment and Modeling." In Pedestrian and Evacuation Dynamics, edited by R. D. Peacock, E. D. Kuligowski, and J. D. Averill, 577-586. Boston, MA: Springer. https://doi.org/10.1007/978-1-4419-9725-8_52.

[4] Stern, R. E., S. Cui, M. L. Delle Monache, R. Bhadani, M. Bunting, M. Churchill, N. Hamilton, et al. 2018. "Dissipation of Stop-and-Go Waves via Control of Autonomous Vehicles: Field Experiments." Transportation Research Part C: Emerging Technologies 89: 205-221. https://doi.org/10.1016/j.trc.2018.02.005.

[5] Kerner, B. S. 2002. "Synchronized Flow as a New Traffic Phase and Related Problems for Traffic Flow Modelling." Mathematical and Computer Modelling 35 (5-6): 481-508. https://doi.org/10.1016/S0895-7177(02)80017-6.

[6] Treiber, M., and D. Helbing. 1999. "Macroscopic Simulation of Widely Scattered Synchronized Traffic States." Journal of Physics A: Mathematical and General 32 (1): L17-L23. https://doi.org/10.1088/0305-4470/32/1/003. U.S. Department of Transportation Federal Highway Administration. 2017. "Next Generation Simulation (NGSIM) Vehicle Trajectories and Supporting Data." https://doi.org/10.21949/1504477.

[7] Yu, H., S. E. Shladover, J. A. Barth, K. Ahn, R. Berthaume, and E. Ferreira. 2021. "Automated Vehicle-Involved Traffic Flow Studies: A Survey of Assumptions, Models, Speculations, and Perspectives." Transportation Research Part C: Emerging Technologies 127: 103101. https://doi.org/10.1016/j.trc.2021.103101.

[8] Chen, D., J. Laval, Z. Zheng, and S. Ahn. 2012. "A Behavioral Car-Following Model That Captures Traffic Oscillations." Transportation Research Part B: Methodological 46 (6): 744-761. https://doi.org/10.1016/j.trb.2012.01.009.

[9] Chen, D., S. Ahn, J. Laval, and Z. Zheng. 2014. "On the Periodicity of Traffic Oscillations and Capacity Drop: The Role of Driver Characteristics." Transportation Research Part B: Methodological 59: 117-136. https://doi.org/10.1016/j.trb.2013.11.005.

[10] Schoenhof, M., and D. Helbing. 2004. "Empirical Features of Congested Traffic States and Their Implications for Traffic Modeling." arXiv preprint cond-mat/0408138.

[11] Ward, J. A., and R. E. Wilson. 2011. "Criteria for Convective Versus Absolute String Instability in Car-Following Models." Proceedings of the Royal Society A: Mathematical, Physical and Engineering Sciences 467 (2132): 2185-2208. https://doi.org/10.1098/rspa.2010.0437.

[12] Wilson, R. E., and J. A. Ward. 2011. "Car-Following Models: Fifty Years of Linear Stability Analysis – a Mathematical Perspective." Transportation Planning and Technology 34 (1): 3-18. https://doi.org/10.1080/03081060.2011.530826.

[13] Wilson, R. E. 2008. "Mechanisms for Spatio-Temporal Pattern Formation in Highway Traffic Models." Philosophical Transactions of the Royal Society A: Mathematical, Physical and Engineering Sciences 366 (1872): 2017-2032. https://doi.org/10.1098/rsta.2008.0018.

[14] Newell, G. F. 2002. "A Simplified Car-Following Theory: A Lower Order Model." Transportation Research Part B: Methodological 36 (3): 195-205. https://doi.org/10.1016/S0191-2615(00)00044-8.

[15] Kerner, B. S. 2004. The Physics of Traffic: Empirical Freeway Pattern Features, Engineering Applications, and Theory. Berlin: Springer.

[16] Treiber, M., and A. Kesting. 2013. Traffic Flow Dynamics: Data, Models and Simulation. Berlin: Springer. https://doi.org/10.1007/978-3-642-32460-4.

[17] Suijs, L. C. W., L. J. J. Wismans, L. Krol, and E. C. Van Berkum. 2015. "Phantom Jam Avoidance Through In-Car Speed Advice." Transportation Research Procedia 8: 227-236. https://doi.org/10.1016/j.trpro.2015.06.057.

[18] Mauch, M., and M. J. Cassidy. 2002. "Freeway Traffic Oscillations: Observations and Predictions." In Transportation and Traffic Theory in the 21st Century, edited by M. A. P. Taylor, 653-672. Oxford: Pergamon.

[19] Ahn, S., and M. J. Cassidy. 2007. "Freeway Traffic Oscillations and Vehicle Lane-Change Maneuvers." In Transportation and Traffic Theory 2007. Papers Selected for Presentation at ISTTT17, edited by R. E. Allsop, M. G. H. Bell, and B. G. Heydecker, 691-710. London: Elsevier.

[20] Ahn, S., J. Laval, and M. J. Cassidy. 2010. "Effects of Merging and Diverging on Freeway Traffic Oscillations: Theory and Observation." Transportation Research Record 2188 (1): 1-8. https://doi.org/10.3141/2188-01.

[21] Krajewski, R., J. Bock, L. Kloeker, and L. Eckstein. 2018. "The highD Dataset: A Drone Dataset of Naturalistic Vehicle Trajectories on German Highways for Validation of Highly Automated Driving Systems." In 2018 21st International Conference on Intelligent Transportation Systems (ITSC), 2118-2125. IEEE. https://doi.org/10.1109/ITSC.2018.8569552.

[22] Nagel, K., and M. Schreckenberg. 1992. "A Cellular Automaton Model for Freeway Traffic." Journal de Physique I 2 (12): 2221-2229. https://doi.org/10.1051/jp1:1992277.

[23] Maerivoet, S., and B. De Moor. 2005. "Cellular Automata Models of Road Traffic." Physics Reports 419 (1): 1-64. https://doi.org/10.1016/j.physrep.2005.08.005.

[24] Nagel, K., and M. Paczuski. 1995. "Emergent Traffic Jams." Physical Review E 51 (4): 2909-2918. https://doi.org/10.1103/PhysRevE.51.2909.

[25] Barlovic, R., T. Huisinga, A. Schadschneider, and M. Schreckenberg. 2002. "Open Boundaries in a Cellular Automaton Model for Traffic Flow with Metastable States." Physical Review E 66 (4): 046113. https://doi.org/10.1103/PhysRevE.66.046113.

[26] Kantelhardt, J. W., M. Fullerton, M. Kämpf, C. Beltran-Ruiz, and F. Busch. 2013. "Phases of Scaling and Cross-Correlation Behavior in Traffic." Physica A: Statistical Mechanics and Its Applications 392 (22): 5742-5756. https://doi.org/10.1016/j.physa.2013.07.024.

[27] Zheng, Z., S. Ahn, D. Chen, and J. Laval. 2011. "Freeway Traffic Oscillations: Microscopic Analysis of Formations and Propagations Using Wavelet Transform." Procedia - Social and Behavioral Sciences 17: 702-716. https://doi.org/10.1016/j.sbspro.2011.04.540.

[28] Nagatani, T. 2002. "The Physics of Traffic Jams." Reports on Progress in Physics 65 (9): 1331-1386. https://doi.org/10.1088/0034-4885/65/9/203.

[29] Khan, Z. H., T. A. Gulliver, W. Imran, K. S. Khattak, A. B. Altamimi, and A. Qazi. 2022. "A Macroscopic Traffic Model Based on Relaxation Time." Alexandria Engineering Journal 61 (1): 585-596. https://doi.org/10.1016/j.aej.2021.06.042.

[30] Eisenblätter, B., L. Santen, A. Schadschneider, and M. Schreckenberg. 1998. "Jamming Transition in a Cellular Automaton Model for Traffic Flow." Physical Review E 57 (2): 1309-1314. https://doi.org/10.1103/PhysRevE.57.1309.

[31] Ahn, S. 2005. "formation And Spatial Evolution Of Traffic Oscillations." Phd Diss., University Of California, Berkeley.

[32] Gasser, I., G. Sirito, and B. Werner. 2004. "Bifurcation Analysis of a Class of 'Car Following' Traffic Models." Physica D: Nonlinear Phenomena 197 (3-4): 222-241. https://doi.org/10.1016/j.physd.2004.07.008.

[33] Klar, A., R. D. Kuhne, And R. Wegener. 1995. "mathematical Models For Vehicular Traffic." Technical Report, University Of Kaiserslautern.

[34] Laval, J., K. B. Amer, and A. Guin. 2009. "Evolution of Oscillations in Congested Traffic: Improved Estimation Method and Additional Empirical Evidences." Transportation Research Record 2124 (1): 41-49. https://doi.org/10.3141/2124-19.

[35] Orosz, G., R. E. Wilson, and G. Stépán. 2010. "Traffic Jams: Dynamics and Control." Philosophical Transactions of the Royal Society A: Mathematical, Physical and Engineering Sciences 368 (1928): 4455-4479. https://doi.org/10.1098/rsta.2010.0205.

[36] Saifuzzaman, M., Z. Zheng, M. M. Haque, and S. Washington. 2017. "Understanding the Mechanism of Traffic Hysteresis and Traffic Oscillations Through the Change in Task Difficulty Level." Transportation Research Part B: Methodological 105: 523-538. https://doi.org/10.1016/j.trb.2017.09.023.

[37] Wagner, P. 2011. "A Time-Discrete Harmonic Oscillator Model of Human Car-Following." The European Physical Journal B 84 (4): 713-718. https://doi.org/10.1140/epjb/e2011-20722-8.

[38] Zhang, T. T., X. Qu, S. Zhang, W. Y. Szeto, and Y. Wang. 2024. "Car-Following Models: A Multidisciplinary Review." arXiv preprint arXiv:2304.07143.

[39] Zielke, B. A., R. L. Bertini, and M. Treiber. 2008. "Empirical Measurement of Freeway Oscillation Characteristics: An International Comparison." Transportation Research Record 2088 (1): 57-67

Journal of Theoretical and Applied Information Technology
15th November 2025. Vol.103. No.21

ISSN: 1992-8645 www.jatit.org E-ISSN: 1817-3195

Annexures:

Table6: The Angular Frequency for Vmax=3 For Different Densities.

Density	0.05	0.1	0.15	0.019
Frequency	0.0042	0.0042	0.0042	0.0042

Table7: The Angular Frequency for Vmax=5 For Different Densities.

Density	0.01	0.05	0.1	0.15
Frequency	0.0045	0.0045	0.0045	0.0045

Table9: The Angular Frequencies for Different α and β Couples for Vmax=5 and P=0.

β \ α	0.1	0.2	0.3	0.4	0.5	0.6	0.7	0.8	0.9
0.1	$\frac{1}{\tau}$	$\frac{2\pi}{T_0}$	$\frac{2\pi}{T_0}$	$\frac{2\pi}{T_0}$	$\frac{2\pi}{T_0}$	$\frac{2\pi}{T_0}$	$\frac{2\pi}{T_0}$	$\frac{2\pi}{T_0}$	$\frac{2\pi}{T_0}$
0.2	$\frac{2\pi}{T_0}$	$\frac{1}{\tau}$	$\frac{2\pi}{T_0}$	$\frac{2\pi}{T_0}$	$\frac{2\pi}{T_0}$	$\frac{2\pi}{T_0}$	$\frac{2\pi}{T_0}$	$\frac{2\pi}{T_0}$	$\frac{2\pi}{T_0}$
0.3	$\frac{2\pi}{T_0}$	$\frac{2\pi}{T_0}$	$\frac{1}{\tau}$	$\frac{2\pi}{T_0}$	$\frac{2\pi}{T_0}$	$\frac{2\pi}{T_0}$	$\frac{2\pi}{T_0}$	$\frac{2\pi}{T_0}$	$\frac{2\pi}{T_0}$
0.4	$\frac{2\pi}{T_0}$	$\frac{2\pi}{T_0}$	$\frac{2\pi}{T_0}$	$\frac{1}{\tau}$	$\frac{2\pi}{T_0}$	$\frac{2\pi}{T_0}$	$\frac{2\pi}{T_0}$	$\frac{2\pi}{T_0}$	$\frac{2\pi}{T_0}$
0.5	$\frac{2\pi}{T_0}$	$\frac{2\pi}{T_0}$	$\frac{2\pi}{T_0}$	$\frac{2\pi}{T_0}$	$\frac{1}{\tau}$	$\frac{2\pi}{T_0}$	$\frac{2\pi}{T_0}$	$\frac{2\pi}{T_0}$	$\frac{2\pi}{T_0}$
0.6	$\frac{2\pi}{T_0}$	$\frac{2\pi}{T_0}$	$\frac{2\pi}{T_0}$	$\frac{2\pi}{T_0}$	$\frac{2\pi}{T_0}$	$\frac{1}{\tau}$	$\frac{2\pi}{T_0}$	$\frac{2\pi}{T_0}$	$\frac{2\pi}{T_0}$
0.7	$\frac{2\pi}{T_0}$	$\frac{2\pi}{T_0}$	$\frac{2\pi}{T_0}$	$\frac{2\pi}{T_0}$	$\frac{2\pi}{T_0}$	$\frac{2\pi}{T_0}$	$\frac{1}{\tau}$	$\frac{2\pi}{T_0}$	$\frac{2\pi}{T_0}$
0.8	$\frac{2\pi}{T_0}$	$\frac{2\pi}{T_0}$	$\frac{2\pi}{T_0}$	$\frac{2\pi}{T_0}$	$\frac{2\pi}{T_0}$	$\frac{2\pi}{T_0}$	$\frac{2\pi}{T_0}$	$\frac{1}{\tau}$	$\frac{2\pi}{T_0}$
0.9	$\frac{2\pi}{T_0}$	$\frac{2\pi}{T_0}$	$\frac{2\pi}{T_0}$	$\frac{2\pi}{T_0}$	$\frac{2\pi}{T_0}$	$\frac{2\pi}{T_0}$	$\frac{2\pi}{T_0}$	$\frac{2\pi}{T_0}$	$\frac{1}{\tau}$

Table10: The Angular Frequencies for Different α and β Couples for Vmax=5 And P=0.5.

β α	0.1	0.15	0.2	0.23	0.26	0.3	0.4	0.5	0.6	0.7	0.8	0.9
0.1	$\frac{1}{\tau}$	$\frac{2\pi}{T_0}$	$\frac{2\pi}{T_0}$	$\frac{2\pi}{T_0}$	$\frac{2\pi}{T_0}$	$\frac{2\pi}{T_0}$	$\frac{2\pi}{T_0}$	$\frac{2\pi}{T_0}$	$\frac{2\pi}{T_0}$	$\frac{2\pi}{T_0}$	$\frac{2\pi}{T_0}$	$\frac{2\pi}{T_0}$
0.2	$\frac{2\pi}{T_0}$	$\frac{1}{\tau}$	$\frac{2\pi}{T_0}$	$\frac{2\pi}{T_0}$	$\frac{2\pi}{T_0}$	$\frac{2\pi}{T_0}$	$\frac{2\pi}{T_0}$	$\frac{2\pi}{T_0}$	$\frac{2\pi}{T_0}$	$\frac{2\pi}{T_0}$	$\frac{2\pi}{T_0}$	$\frac{2\pi}{T_0}$
0.3	$\frac{2\pi}{T_0}$	$\frac{2\pi}{T_0}$	$\frac{1}{\tau}$	$\frac{2\pi}{T_0}$	$\frac{2\pi}{T_0}$	$\frac{2\pi}{T_0}$	$\frac{2\pi}{T_0}$	$\frac{2\pi}{T_0}$	$\frac{2\pi}{T_0}$	$\frac{2\pi}{T_0}$	$\frac{2\pi}{T_0}$	$\frac{2\pi}{T_0}$
0.4	$\frac{2\pi}{T_0}$	$\frac{2\pi}{T_0}$	$\frac{2\pi}{T_0}$	$\frac{1}{\tau}$	$\frac{2\pi}{T_0}$	$\frac{2\pi}{T_0}$	$\frac{2\pi}{T_0}$	$\frac{2\pi}{T_0}$	$\frac{2\pi}{T_0}$	$\frac{2\pi}{T_0}$	$\frac{2\pi}{T_0}$	$\frac{2\pi}{T_0}$
0.5	$\frac{2\pi}{T_0}$	$\frac{2\pi}{T_0}$	$\frac{2\pi}{T_0}$	$\frac{2\pi}{T_0}$	$\frac{1}{\tau}$	$\frac{2\pi}{T_0}$	$\frac{2\pi}{T_0}$	$\frac{2\pi}{T_0}$	$\frac{2\pi}{T_0}$	$\frac{2\pi}{T_0}$	$\frac{2\pi}{T_0}$	$\frac{2\pi}{T_0}$
0.6	$\frac{2\pi}{T_0}$	$\frac{2\pi}{T_0}$	$\frac{2\pi}{T_0}$	$\frac{2\pi}{T_0}$	$\frac{1}{\tau}$	$\frac{2\pi}{T_0}$	$\frac{2\pi}{T_0}$	$\frac{2\pi}{T_0}$	$\frac{2\pi}{T_0}$	$\frac{2\pi}{T_0}$	$\frac{2\pi}{T_0}$	$\frac{2\pi}{T_0}$
0.7	$\frac{2\pi}{T_0}$	$\frac{2\pi}{T_0}$	$\frac{2\pi}{T_0}$	$\frac{2\pi}{T_0}$	$\frac{1}{\tau}$	$\frac{2\pi}{T_0}$	$\frac{2\pi}{T_0}$	$\frac{2\pi}{T_0}$	$\frac{2\pi}{T_0}$	$\frac{2\pi}{T_0}$	$\frac{2\pi}{T_0}$	$\frac{2\pi}{T_0}$
0.8	$\frac{2\pi}{T_0}$	$\frac{2\pi}{T_0}$	$\frac{2\pi}{T_0}$	$\frac{2\pi}{T_0}$	$\frac{1}{\tau}$	$\frac{2\pi}{T_0}$	$\frac{2\pi}{T_0}$	$\frac{2\pi}{T_0}$	$\frac{2\pi}{T_0}$	$\frac{2\pi}{T_0}$	$\frac{2\pi}{T_0}$	$\frac{2\pi}{T_0}$
0.9	$\frac{2\pi}{T_0}$	$\frac{2\pi}{T_0}$	$\frac{2\pi}{T_0}$	$\frac{2\pi}{T_0}$	$\frac{1}{\tau}$	$\frac{2\pi}{T_0}$	$\frac{2\pi}{T_0}$	$\frac{2\pi}{T_0}$	$\frac{2\pi}{T_0}$	$\frac{2\pi}{T_0}$	$\frac{2\pi}{T_0}$	$\frac{2\pi}{T_0}$

ISSN: 1992-8645 www.jatit.org E-ISSN: 1817-3195

Table11: The Angular Frequency and The Traffic Phase for The Couple (α, β) (a) for I-80 (b) US-101

(a)

α	β	frequency	Phase
0.99	0.97	$2\pi/T_0$	Jam
0.98	0.96	$2\pi/T_0$	Jam
0.88	1.0	$2\pi/T_0$	Jam
1.0	0.27	$1/\tau$	Congestion
0.92	0.95	$2\pi/T_0$	Jam
0.62	0.75	$2\pi/T_0$	Jam
0.91	0.80	$2\pi/T_0$	Jam
0.90	0.86	$2\pi/T_0$	Jam
0.61	0.70	$2\pi/T_0$	Jam

(b)

α	β	frequency	Phase
1.0	1.0	$2\pi/T_0$	jam
0.97	0.98	$2\pi/T_0$	Jam
0.84	0.87	$2\pi/T_0$	Jam
0.26	0.86	$1/\tau$	Congestion
0.26	0.83	$1/\tau$	Congestion
0.76	0.83	$2\pi/T_0$	Jam
0.24	0.84	$1/\tau$	Congestion
0.29	0.81	$1/\tau$	Congestion
0.29	0.84	$1/\tau$	Congestion

Table 15: The Mean Speed and The Mean Headway for Vmax=5 P=0 and K=0.7

Time	*All iterations*	*1 T_0*	*2 T_0*	*7T_0*	*8T_0*	*9T_0*	*10T_0*
Mean speed	*0.3*	*0.29*	*0.30*	*0.30*	*0.29*	*0.30*	*0.30*
Mean space headway	*23.94*	*24.35*	*24.25*	*23.61*	*24.62*	*23.28*	*24.00*

Table 16: The Mean Speed and The Mean Headway for Vmax=5 P=0.5 and K=0.7

Time	All iterations	1 T_0	2 T_0	7T_0	8T_0	9T_0	10T_0
Mean speed	0.5	0.50	0.49	0.50	0.49	0.50	0.49
Mean space headway	47.46	46.42	48.50	48.64	47.95	48.02	46.90

Table 14. the mean speed and the mean headway for the recording number 03 in the HighD dataset

Time	Full recording	$7T_0$	$8T_0$	$9T_0$	$10T_0$
Mean speed(m/s)	31.80	32,85	30.88	31.77	31.77
Mean space headway(m)	76.32	73.17	75.39	78.99	86.01

Table12: Mean Speed and The Mean Space Headway for The Recording I-80 from5:15 to 5:30.

Time	Full recording	$1T_0$	$2T_0$	$3T_0$	$4T_0$
Mean speed(ft/s)	14.60	12.30	16.55	15.74	9.72
Mean space headway (ft)	44.5	36.48	55.19	50.05	35.51

Table13: The Mean Speed and The Mean Space Headway for The Recording US-101 From 7:50 To 8:05.

Time	Full recording	$1T_0$	$2T_0$
Mean speed(ft/s)	39.60	42.63	40.48
Mean space headway (ft)	77.28	81.44	77.93